TESCAN

A unique combination of Plasma FIB and field-free UHR SEM for the widest range of multiscale materials characterization applications

1 mm cross-section through a Li-ion battery electrode

TESCAN AMBER X

- ✓ High throughput, large area FIB milling up to 1 mm
- ✓ Ga-free microsample preparation
- ✓ Ultra-high resolution, field-free FE-SEM imaging and analysis
- ✓ In-column SE and BSE detection
- ✓ Spot optimization for high-throughput, multi-modal FIB-SEM tomography
- ✓ Superior field of view for easy navigation
- ✓ Essence™ easy-to-use, modular graphical user interface

For more information visit

www.tescan.com

ADVANCED ENERGY MATERIALS
www.advenergymat.de

Industrial Fabrication of 3D Braided Stretchable Hierarchical Interlocked Fancy-Yarn Triboelectric Nanogenerator for Self-Powered Smart Fitness System

Ronghui Wu, Sai Liu, Zaifu Lin, Shuihong Zhu, Liyun Ma, and Zhong Lin Wang**

Sustainable, clean, random energy resources from the environment, like that from ubiquitous human biomechanical movements, are highly desirable for the information era. Such biomechanical energy can be captured via textile triboelectric nanogenerators (TENGs). However, realizing a textile TENG that has a self-driven working mode, dynamic pattern designability, high electrical performance, mechanical robustness, and industrialized fabrication is challenging because of the difficulty in fancy-yarn structure manipulation. Here, for the first time, a 3D braided stretchable hierarchical interlocking fancy-yarn TENG (3D HIFY-TENG) with deoxyribonucleic acid-like double-wing spiral structure is industrially exploited for multifunctional energy harvesting modes and self-powered biomechanical sensing. The 3D HIFY-TENG can generate self-driven triboelectrical outputs without relying on other objects by body movements. It shows a mechanical robustness (6.9 cN dtex^{-1}), excellent stretchability (>350%), weavability, washability and human-body comfort. Moreover, geometric and mechanical behavior of the 3D HIFY-TENG are systematically investigated theoretically and experimentally. Further, multifunctional 3D HIFY-TENG fabrics are explored, which can not only harvest biomechanical energy and monitor body movement, but exhibit a unique adjustable pore effect, providing potential for dynamic electronic textile pattern design. In addition, a smart fitness system is developed for exercise management of real-time exercise detection, frequency analysis, and self-powered posture correction alarms.

1. Introduction

In the era of rapid development of the Internet of Things (IoT), 5G and intelligent devices, sustainable, clean, ubiquitous energy resources from the environment are highly desirable.[1] Such energy resources, like that from human body movement, can be captured using textile-based triboelectric nanogenerators (TENGs) for energy harvesting[2] and human versatile sensing.[3] As a basic unit of textile TENG, yarn TENG can not only be directly weaved or knitted into breathable, flexible, lightweight clothes,[4] but also ubiquitously harvest energy from body movements[5] and monitor human biomechanical and physiological signals,[6] showing great application prospects in smart life.[7] However, the further advancement of yarn TENGs still faces several critical challenges. First, current yarn TENGs normally have an isotropic core-sheath structure,[8] with electrode fibers in the middle and dielectric fibers wrapping as the sheath layer.[9] This architecture does not fully exploit the advantages of yarn structure, and only allows fibers assembled in a 1D direction,[10] which limits the freedom of single yarn movement, thereby restricting the yarn full function of TENG for energy harvesting and sensing. Second, a majority of fabric TENG can only generate electricity on the condition of contacting other objects, two or more fabrics are required to form contact sliding or contact separation movement.[9,11] Third, the fabrication of yarn TENG, such as coating,[11a,12] is difficult to maintain an even surface because of the Reynolds instability.[13] The uneven yarns will limit the breathability, flexibility, and stretchability of the fabric TENG.[14] Forth, some yarns with large diameters greatly restrict the degree of freedom, softness, comfort, and possibility of applicability of the fabric.[15] Therefore, developing an all-fiber 3D yarn TENG with controllable structure, applicable diameter, and multi-responsive energy harvesting working mode will be of great significance to expanding the development and application of textile electronics.

To address the aforementioned problems, yarn TENGs with unconventional structures and styles,[16] that is, fancy yarns,[17] which can assemble fibers with different Young's modulus,

R. Wu, L. Ma, Z. L. Wang
Beijing Institute of Nanoenergy and Nanosystems
Chinese Academy of Science
Beijing 101400, China
E-mail: maliyun0323@hotmail.com; zlwang@binn.cas.cn
S. Liu
College of Textile Science and Engineering (International Institute of Silk)
Zhejiang Sci-Tech University
Hangzhou 310018, China
R. Wu, Z. Lin, S. Zhu, L. Ma
College of Physical Science and Technology
Fujian Provincial Key Laboratory for Soft Functional Materials Research
Xiamen University
Xiamen 361005, China
The ORCID identification number(s) for the author(s) of this article can be found under https://doi.org/10.1002/aenm.202201288.

DOI: 10.1002/aenm.202201288

stretchability, electrical conductivity, and insulation properties into a single yarn will be a good solution. Fancy yarns are widely developed for multifunctional textiles,[18] because they can obtain desired functional yarns by positioning wrapping and precise embedding of functional fiber materials on the designated yarns in a continuous and controlled manner. For example, lace fancy yarns with a bamboo section shape have been developed to enhance wound dressings.[19] In addition, the fancy yarns with multi-functional composite are novel in pattern, unique and delicate in style,[20] and have different visual effects.[21] The unconventional shape characteristics will also enable the yarns with adjustable mechanical properties, thermal conductivities, electrical properties, and unique shape operability.[22] However, though fancy-yarns have been widely applied in technical and biomedical textiles, few researches have been carried out regarding energy harvesting textiles yet.

Here, for the first time, a novel and multifunctional 3D braided stretchable hierarchical interlocked fancy-yarn TENG (3D HIFY-TENG), with a hierarchical double-wing structure is introduced. The double semicircle wing all-fiber yarns interlocked on both sides of a torso, that is, polyurethane (PU) yarns. Each wing yarn has a primary core–shell structure with conductive silver-coated polyamide (PA) yarn as the core part and insulated yarns as the shell part. Owing to the unique hierarchical interlocked structure, the wings of the 3D HIFY-TENG contact and separate with the PU yarn under a stretching state and recovery state, generating a tribo-electrical signal. In addition, the 3D HIFY-TENG generates an energy signal when contacting with human skin, allowing multi-form energy harvesting modes. In addition, we developed a numerical model to verify and predict the motion trajectories of wing yarns in 3D HIFY-TENG, which shows good consistency with the experimental results. Besides, the 3D HIFY-TENG is further weaved into self-powered fabric sensor with a plain structure, which has a much higher stretchability compared to the fabric fabricated with normal core–shell structured yarn TENG.[23] Moreover, a smart fitness system is developed by integrating the fancy yarn into a smart yoga belt, for multifunctional exercise management of exercise frequency statistical analysis, real-time exercise detection, and self-powered posture correction alarming.

2. Results and Discussion

Industrial-scalable processing, fast working speed, and low-cost braiding method was used for 3D HIFY-TENG fabrication, as shown in **Figure 1**a and Figure S1, Supporting Information. In the 3D HIFY-TENG, polyurethane (PU) yarn is used as the torso yarns for stabilizing the wing yarns into an anisotropic interlocked manner (Figure 1a(i)), because of its excellent elasticity and stretchability. Wing yarns are core–shell structured yarns, consisting of conductive core yarn and insulating shell yarn, prepared by a mass-productive twisting method. For the conductive core yarn, polyamide (PA) yarn coated with silver layer was used because of its high electrical conductivity. For the insulating shell yarn, polyester (PET), polyimide (PI), and PA yarns are chosen because they are the most commonly worldwide used synthetic yarns with good electrical insulation, low fabrication cost, and high production efficiency. The shell yarns are wrapped on the surface of core yarns with a high covering rate. Before fabrication, two bobbins with PU yarns are fixed on the holders that rotate clockwise, while another two bobbins of core–shell structured wing yarns are symmetrically put on the holders that rotate counterclockwise. During fabrication processing, the holders run in a programmed rotating trajectory (Figure 1a(ii)), enabling two groups of yarns to meet and interlace in the braiding area, forming a 3D interlocked structure with two wing yarns being stabilized by the torso yarns, as shown in Figure 1a(i). Afterward, the prepared composite yarns are fed into the rollers for tension adjusting before collecting on the final bobbins. The braiding process has a fast-working speed, and ≈400–800 m of the 3D HIFY-TENG TENG can be obtained on a one-ring bobbin within 1 h (Video S1, Supporting Information). As shown in Figure 1b, the unlimited length of 3D HIFY-TENG with a uniformed structure can be easily fabricated by the abovementioned preparing strategy. The 3D HIFY-TENG has an interlocked structure, where two PU yarns are processed with S twisting into a DNA-like double spiral structure, embedding the wing yarns in the middle at each unit twist, while two wing yarns naturally form inclined semicircular loops that are distributed on double sides to maintain a tension balance, as shown in Figure 1c,d. It is worth mentioning that in each type of wing yarn, the conductive yarn electrodes are uniformly and continuously wrapped by insulating yarns (PET, PI, and PA yarns), as shown in Figure 1e and Figure S2, Supporting Information.

According to the inherent properties of yarns in textiles, as a basic unit of textile TENG, 3D HIFY-TENG can naturally be weaved into textiles for wearable self-powered sensors and energy harvesters. Depending on the textile pattern design, the fabric can be woven into any size and pattern without sacrificing fabric softness and omnidirectional flexibility (Figure 1f). In addition, the 3D HIFY-TENG also can be sewn on a specific position of the fashion garment as a fancy yarn for decoration and inspection. The 3D HIFY-TENG has a big deformation and excellent recovery ability under external forces, enabling the double wing yarns and the PU yarns to contact and separate during the stretching and recovery process, generating an electrical signal. Therefore, 3D HIFY-TENG can be used in self-powered stretching and pressing sensors, such as smart elastic belts for multifunctional exercise management of exercise frequency statistical analysis, real-time exercise detection, and self-powered posture correction alarming (Figure 1g).

The functionality of the yarn is realized by engineering the structure and shape of the fibers.[24] To realize a self-driven fancy yarn TENG, a yarn structure with big deformability that induces contact and separation between different fiber components is essential. In our design, the detailed self-driven structure of this 3D HIFY-TENG is illustrated in **Figure 2**a. Because of the high stretchability and elasticity of the PU torso yarns, as well as the hierarchical interlocked structure of the wing yarns, the 3D HIFY-TENG shows a unique stretchability, deformability, and resilience. The geometric morphology of the wing yarns is similar to a sinusoidal with periodicity. When 3D HIFY-TENG was stretched to 60%, the pitch (h) of the DNA-like double spiral structured PU torso yarn gradually enhances, leading the curvature of the bulging wing yarns to decrease (Figure 2b). When the 3D HIFY-TENG is stretched to 120%,

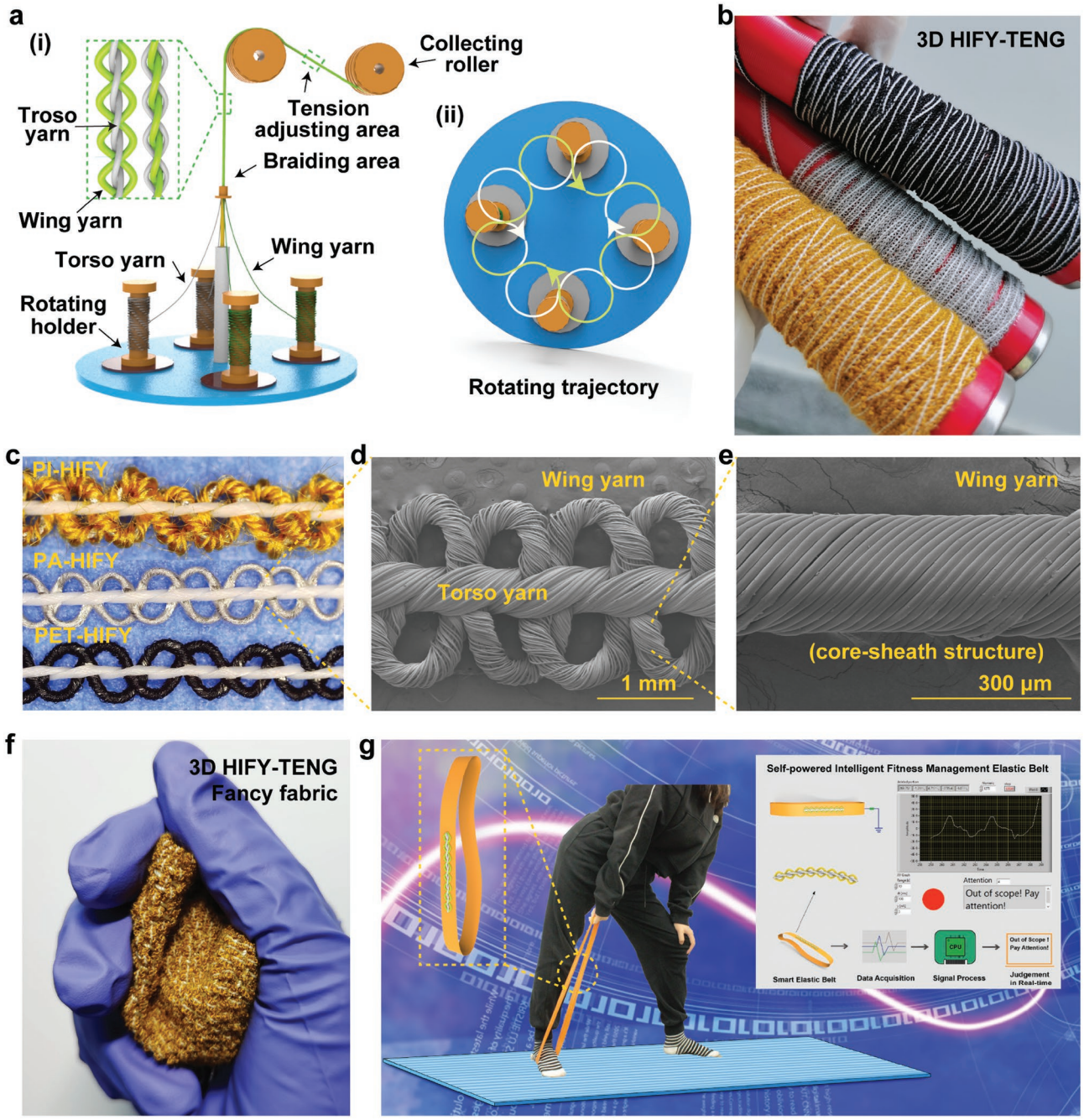

Figure 1. 3D braided hierarchical interlocked fancy-yarn for self-powered smart fitness system. a) Fabrication process of the 3D HIFY-TENG (i), which is formed by rotating the plates according to the programmable designed trajectory (ii). b) Images of the as-prepared 3D HIFY-TENG on the bobbins. c) Microscope images of the 3D HIFY-TENG with different wrapping yarns, that is, polyimide (PI), polyamide (PA), and polyester (PET). d) SEM image of the hierarchical 3D HIFY-TENG, with double wing yarns stabilized by a torso yarn, that is, polyurethane (PU) yarn. e) SEM image of a core–shell structured wing yarn. f) Image of the 3D HIFY fabric with plain weaving structure. g) Illustration of the smart fitness system with self-powered yoga belt (i) and real-time monitoring display (ii).

the double wings are fully straightened, making the wing yarns in contact with the torso yarns (Figure 2b). When the strain was released, the 3D HIFY-TENG will recover to the original state owing to the high elasticity of PU yarns and the DNA-like double spiral structure, making the wing yarns and torso yarns separate. In Figure 2c, the radial strain variation of 3D HIFY-TENG during stretching was characterized by the electron microscope. The geometric diameter of 3D HIFY-TENG dramatically decreases until it reaches a contact point, where the wing yarns are completely touched with the torso yarns. The 3D HIFY-TENG with different wrapping yarns, that is, PI, PA, and PET, are named PI-HIFY, PA-HIFY, and PET-HIFY, respectively. Three kinds of 3D HIFY-TENG show a similar tendency of geometric changing during stretching, but the strains at contact

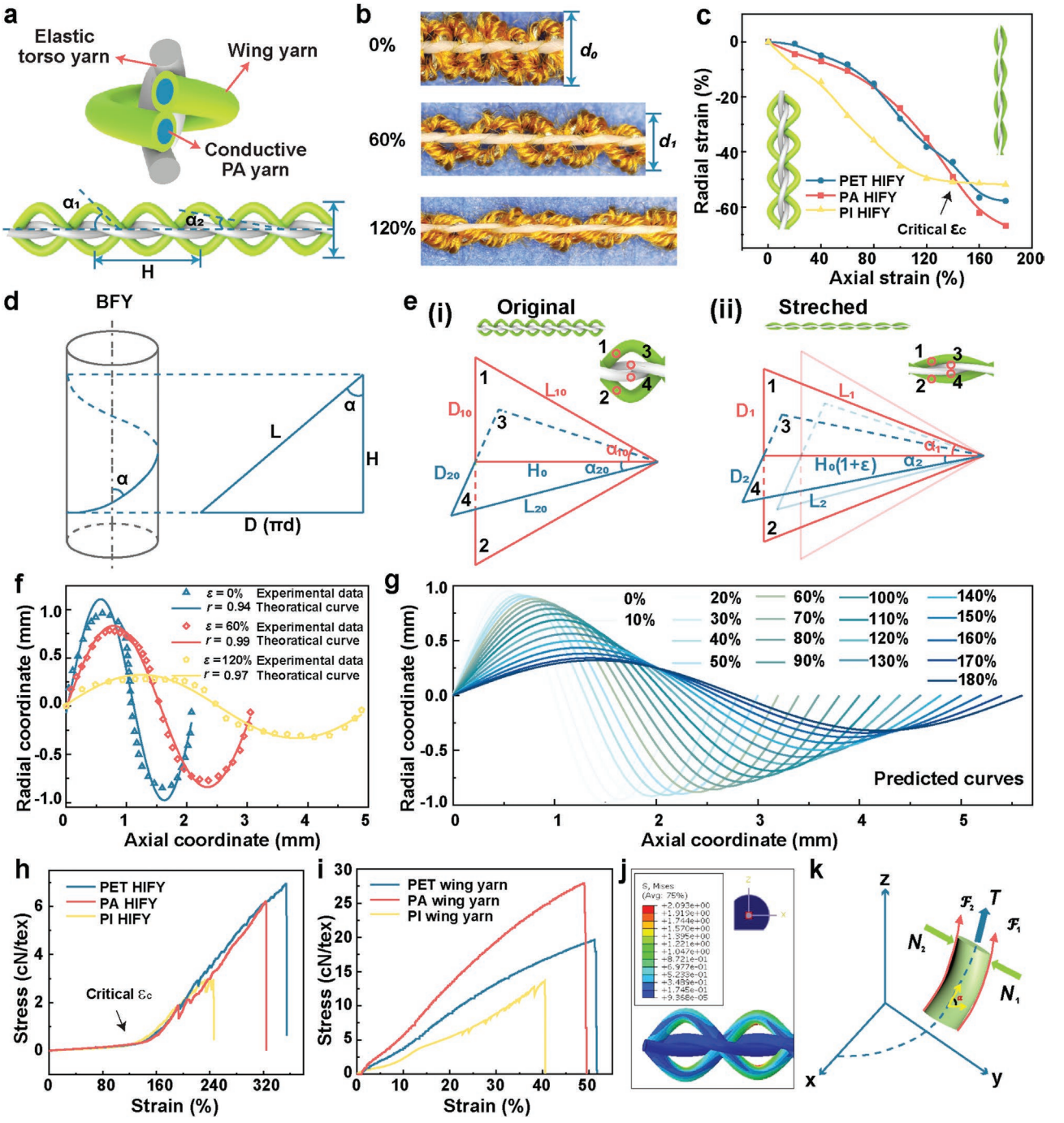

Figure 2. Experimental and theoretical analysis of the geometric and mechanical behavior of a 3D HIFY-TENG. a) Illustration of the 3D HIFY-TENG from cross-sectional and side view. b) 3D HIFY-TENG being stretched to 0%, 40%, and 120% elongation, showing excellent deformation ability under axial stretching. c) Variation of the radial strains when 3D HIFY-TENGs with different wrapping yarns are stretched from 0% to 180%. d) Illustration of the unfolding of one spiral wing yarn. e) Geometric unfolding illustration of the wing and torso yarns before (i) and after (ii) stretching. D_{10}, L_{10}, α_{10}, and D_{20}, L_{20}, α_{20} in (e-i) mean the initial state of geometric parameters of the wing yarn and torso yarn, respectively. D_1, L_1, α_1, and D_2, L_2, α_2 in (e-ii) mean the stretched state of geometric diameter of the wing yarn and torso yarn, respectively. f) Experimental data and theoretic curves of the wing yarns of 3D HIFY-TENG at different stretching strain of 0%, 60% and 120%. g) Predicted trajectory of the wing yarns at different strain range from 0% to 180%. h) Typical mechanical stretching behaviors of the 3D HIFY-TENG, which can be divided into two stages of gentle increasing and fast increasing. i) Typical mechanical stretching behaviors of the wing yarns of 3D HIFY-TENGs. j) Tension distribution of the 3D HIFY-TENG, predicted by finite element analysis via ABAQUS software. k) Force analysis diagram of the wing yarns.

points for PA-HIFY and PET-HIFY are bigger than PI-HIFY. Like the aforementioned, with the stretching and releasing, the contacts and separation between the wing yarns and torso yarns enable 3D HIFY-TENG with electrical outputs.

A theoretical numerical model is further developed and used to analyze and verify the geometric deformation of the 3D HIFY-TENG. As shown in Figure 2d, the pitch (H) and wrapping angle (α) of the wrapping yarn has the following relationship:

$$H = L_1\cos\alpha_1 = L_2\cos\alpha_2 \tag{1}$$

where L_1, L_2 are the track length of wing yarns and torso yarns. α_1, α_2 are the wrapping angle of wing yarns and torso yarns, respectively. In 3D HIFY-TENG, wing yarns and torso yarns share the same pitch length H (Figure 2a). When the 3D HIFY-TENG is stretched to strain ε, the wing yarns and torso yarns obey the helical path, while the helical distance of one unit helix increases from initial length H_0 to H_0 (1+ε), as illustrated in Figure 2e. The coordinates from the optical images of the 3D HIFY-TENG at different stretching states of 0%, 60%, and 120% are first fitted with sine functions, as shown in Figure 2f. The fitted curves show a good consistency with the experimental data, which means the tensile geometry of the wing yarns of 3D HIFY-TENG fits well with the proposed sinusoidal. The curve equation can be derived into

$$y = D\sin\left(2\pi x/\left(H_0\left(1+\varepsilon\right)\right)\right) \tag{2}$$

where D is the diameter of the HIFY, H_0 is the initial wrapping angle of wing yarns, ε is the axial strain. Based on the ordinate values of the peak positions of HIFY (Figure S3, Supporting Information), we have a characteristic curve as follow:

$$D = 0.98 - 0.39\varepsilon + 0.91\varepsilon^2 - 1.07\varepsilon^3 + 0.32\varepsilon^4 \tag{3}$$

By combining Equations (2) with (3), we can get the predicted trajectory curves of the HIFY

$$y = \left(0.98 - 0.39\varepsilon + 0.91\varepsilon^2 - 1.07\varepsilon^3 + 0.32\varepsilon^4\right)\sin\left(2\pi x/\left(H_0\left(1+\varepsilon\right)\right)\right) \tag{4}$$

When the diameter of the HIFY is equal with the diameter of wing yarns and torso yarns, the wing yarns fully contact with the torso yarns. That is

$$D_{\varepsilon=\varepsilon_c} = 2d_1 + 2d_2 \tag{5}$$

where ε_c is the critical contacting strain, d_1 and d_2 are the diameter of wing and torso yarns.

Based on the promoted model, we calculate the critical contacting strain (ε_c) of the 3D HIFY-TENG, which is in the range of ≈120–130%, which shows a consistent value with the experimental data. Further, by invoking Equation (4), we can get the predicted moving trajectory of 3D HIFY-TENG under different stretching strains from 0% to 180%, as shown in Figure 2g. It is obvious that with the strain increasing, the amplitude decreases and the period increase simultaneously. The theoretical model provides important meaning for predicting the geometric deformation of the 3D HIFY-TENG.

To further verify the big geometric deformability of 3D HIFY-TENG, stretching testing is carried out and mechanical performance is analyzed and studied in Figure 2h. The mechanical stress–strain curve involves into two different stages, divided by the contact point. In the initial strain range (0–100%), 3D HIFY-TENG shows a very low modulus of 0.2 cN tex^{-1}, which is much lower than that of the wing yarns (Figure 2i; Figure S4, Supporting Information). It enables 3D HIFY-TENG excellent flexibility, softness, and conformability with human bodies within this range. When a stretching force is applied, the stress on the 3D HIFY-TENG is applied to the extension of PU torso yarns and the straightening of the wing yarns, which can be also verified by the finite element analysis results, as shown in Figure 2j. With strain increasing, the friction forces between the torso yarns and wing yarns enable wing yarns to be straightening from bending, as shown in the force analysis diagram in Figure 2k. After the stretching strain reach the critical contacting strain ε_c, that is, contact point, wing yarns get fully straightened, more stress is needed for the extension of both PU yarns and the wing yarns. As the Young's modulus of the wing yarns are much bigger than the PU torso yarns (Figure 2i; Figure S5, Supporting Information), the modulus for 3D HIFY-TENG increases rapidly after the contact point (Figure 2h). Due to the geometric characteristics and the high stretchability of PU yarns, the 3D HIFY-TENGs exhibit a big breaking elongation, as shown in Figure 2h. PI-HIFY, PET-HIFY, and PA-HIFY shows breaking elongation of 245%, 323%, and 354%, respectively.

Because of the unique geometric structure of the 3D HIFY-TENG deformation, every stretching and recovery of the 3D HIFY-TENG will induce c and separation between wing yarns and torso yarns (**Figure 3**a). Here, the yarn stretching and recovery is controlled by a linear motor. Owing to the difference in electron affinity potential energies of the two kinds of yarns, each 3D HIFY-TENG can work as a stretchable self-support single-electrode TENG. The working principle is illustrated in Figure 3b. Take PI HIFY-TENG as an example, when the 3D HIFY-TENG is stretched, the PI yarns from wing yarns get in contact with the PU torso yarns, and the negative charge is transferred from the PI yarns to the PU yarns owing to the different surface electron affinity, as shown in Figure 3b(i). Subsequently, when the stretching force is released, the wing yarns get separated from PU torso yarns, and an electric potential difference occurs. The positive charges on the PI layer will prompt negative charges on the wing yarns for compensation, thereby forcing free electrons from the ground to the PA conductive yarns, as illustrated in Figure 3b(ii). When the PU yarn is completely separated from the wing yarns, the charges are in equilibrium and no electrons transformation occurs at this stage (Figure 3b(iii)). As shown in Figure 3b(iv), when the 3D HIFY-TENG is stretched again, the PI wing yarns approach the PU yarn again, leading to opposite electrons from the ground to PA conductive yarns until the PU yarns and PI wing yarns completely contact. As a result, alternating electricity is generated through periodic stretching and recovering of the 3D HIFY-TENG. The potential distributions of the PI and PU layers during touching and separating states are simulated by COMSOL. As exhibited in Figure S6, Supporting Information, an obvious positive potential is observed on the surface of PU yarn after separation from contacting, which is consistent with the aforementioned analyzed working principle. Therefore, the 3D HIFY-TENG can be stretched into a big deformation to harvest biomechanical energy from human movement (Figure 3c).

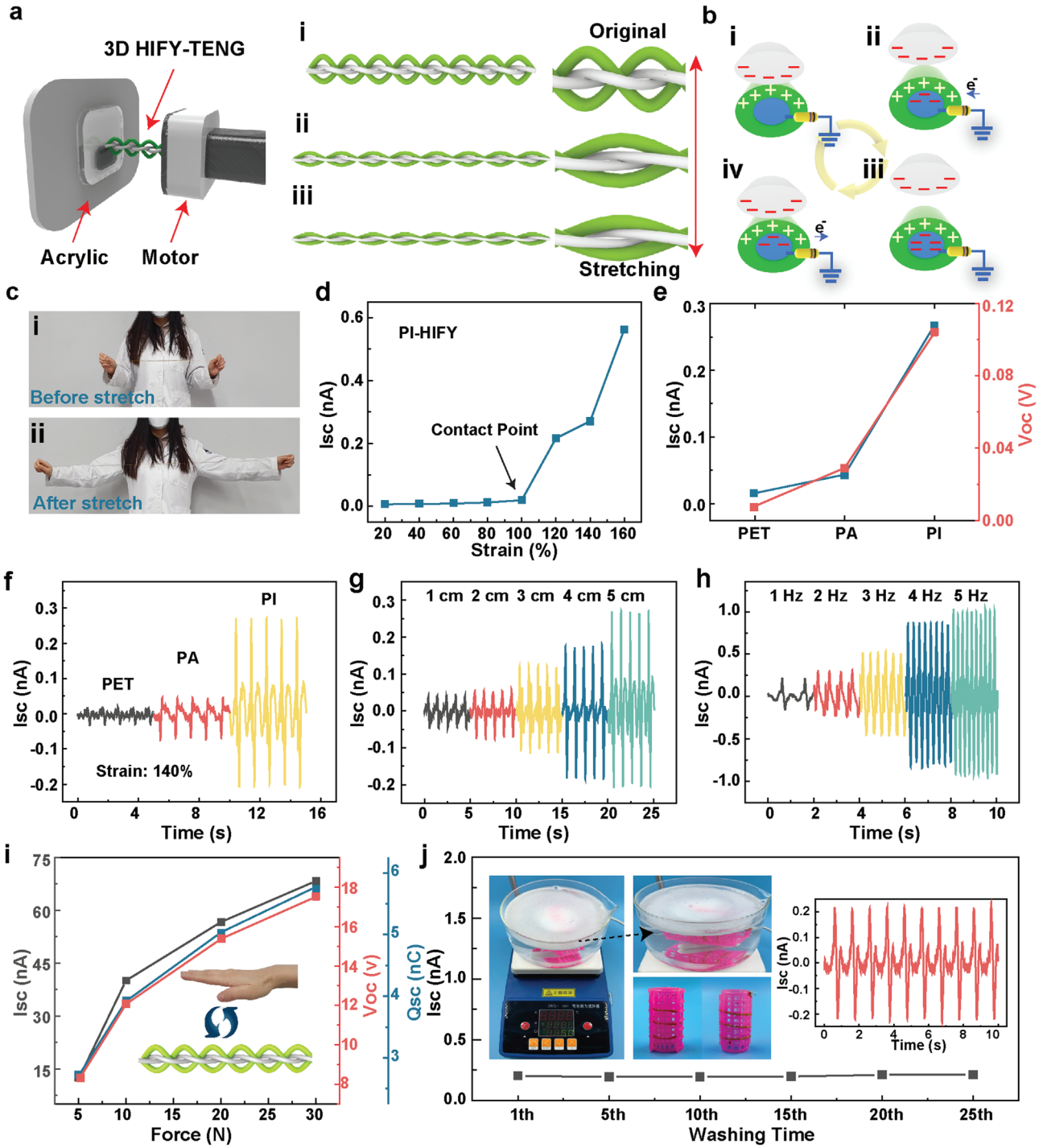

Figure 3. Electrical outputs of 3D HIFY-TENG under stretching and tapping modes. a) Illustration of the stretching applying equipment and the deformation of 3D HIFY-TENG. b) Working mechanism for the 3D HIFY-TENG during stretching and recovery. c) The 3D HIFY-TENG shows a big stretchability and deformability for human body biomechanical energy harvesting. d) The short-circuit current (I_{sc}) of the 3D HIFY-TENG when stretched to 160% strain, showing a big increment in energy output after the contacting point of the 3D HIFY-TENG. e) I_{sc} and h) open-circuit current (V_{oc}) when 3D HIFY-TENG with different wrapping yarn components (PET, PA, PI) were stretched to 140%. f) The I_{sc} of the 3D HIFY-TENG with different wrapping yarn components (PET, PA, PI) while repeating for five times. g) Energy output of 3D PI HIFY-TENG with different length (1–5 cm). h) Energy output of 3D HIFY-TENG under mechanical frequency range 1–5 Hz. i) Energy output under pressing working mode. j) Washability test of 3D HIFY-TENG. Insets are the images of samples during washing tests with detergent, and the continuous energy output after 25 times washing.

In Figure 3d, the 3D HIFY-TENG shows an obvious increasing energy output when it is stretched into 120% strain. With the strain increasing, the contact force between wing yarns and PU torso yarns enhances, resulting in a higher energy output.

Among the three kinds of 3D HIFY-TENG with different wrapping yarns, PI HIFY has a highest output performance, which is because of a high electron affinity potential energy of PI yarns compared to PET and PA yarns (Figure 3e,f and Figure S7a, Supporting Information). The output performance of PI HIFY with different lengths (1–5 cm) is characterized under 1 Hz stretching and recovering condition (Figure 3g; Figure S7b, Supporting Information). As predicted, the output performance of the 3D HIFY-TENG rises with length increment. To better verify the practical application of 3D HIFY-TENG in human body biomechanical energy harvesting, we measured the response to the mechanical frequencies of common human motions (1–5 Hz). 3D HIFY-TENG exhibits a good and stable response to these mechanical frequencies, as shown in Figure 3h and Figure S7c,d, Supporting Information. Moreover, the 3D HIFY-TENG shows an excellent cyclic stability under 110 times consecutive stretching and recovery, as shown in Figure S8, Supporting Information. What is more, the output power and charging behavior of 3D HIFY-TENG are investigated in Figure S9, Supporting Information.

Apart from self-driven stretching modes, 3D HIFY-TENG can also generate electrical energy in pressing mode with high energy output. Taking human skin as an example, an electrical signal will generate during contact and separation because of the electron affinity potential energies difference between human skins and PI yarns. The working principle for pressing TENG is also single electrode mode TENG, where the conductive PA yarns work as the electrodes, and the PI wrapping yarns act as the friction layer. The electrical performance of PI 3D HIFY-TENG, PET 3D HIFY-TENG, and PA 3D HIFY-TENG in pressing mode are investigated and compared. PI 3D HIFY-TENG shows a highest energy harvesting ability among the three kinds of TENG (Figure S10a–c, Supporting Information), which is consistent with results in self-driven stretching working mode. With the pressure increasing from 5–30 N, the energy output keeps increasing from 12.2 nA, 8.2 V and 2.7 nC to 68 nA, 17.5 V and 5.8 nC, as shown in Figure 3i and Figure S10d–f, Supporting Information. Moreover, 3D HIFY-TENG also shows a good response to mechanical tapping with different mechanical frequencies (0.5–2.5 Hz), as well as good cyclic stability under 1000 times consecutive loading and unloading (Figures S10g–i and S11, Supporting Information). Considering textiles are apt to contact with human bodies and other objects, energy harvesting during pressing mode will enable textiles to harvest energy from human body mechanical movement, which is normally wasted and widely dispersed energy. Therefore, this multi-functional 3D HIFY-TENG with different working modes (self-driven stretching mode and pressing mode) will help to harvest energy conveniently and efficiently.

Washability is another important indispensable property for electronic textiles because of the complex and wearable application conditions and scenarios. Thus, the washability of 3D HIFY-TENG is tested by washing with detergent. As shown in Figure 3j, the 3D HIFY-TENG is wound around the hollowed-out holder, allowing it to fully contact with water and detergent during the washing process, so that the 3D HIFY-TENG can be fully washed. The 3D HIFY-TENG are immersed and stirred for 30 min for fully washing. After drying, the 3D HIFY-TENG yarn is sturdy and robust as no grinning was noticed even after 25 times of washing, and the energy output of the 3D HIFY-TENG shows no obvious change after every washing steps. The electrical response to the yarn stretching and recovery are stable and effective, meaning the 3D HIFY-TENG can be used for long-term wearable textile energy harvesters.

3D HIFY-TENG with good stretching and recovery property, mass productivity, and good flexibility can meet various mechanical requirements and conditions of further industrial-scalable fabric fabrication processing, such as weaving, knitting, and tailoring. As shown in **Figure 4**a–e and Figure S12, Supporting Information, three kinds of 3D HIFY-TENGs (PI, PET, PA) are weaved into fabrics with a plain structure. Here, commercialized PA yarns are selected as weft yarns, and 3D HIFY-TENGs are fed into the weaving machine with designed pattern, as illustrated in Figure 4c. The 3D HIFY-TENG fabric shows a good flexibility, bendability, and conformity (Figure 4d). As shown in Figure 4f, the 3D PI HIFY-TENG has a lower weft density (6 counts cm^{-1}) than the other two HIFY-TENG, which can be also seen from the microscopic images in Figure S13, Supporting Information. Meanwhile, three kinds of 3D HIFY-TENGs (PI, PET, PA) have a similar warp density (≈3.8 counts cm^{-1}), which is determined by the fixed weaving reed density (Figure 4b). Because of the unique double-wing interlocked structure of 3D HIFY-TENG, the weft density is lower than normal weaved plain-structure textiles. As discussed in the aforementioned mechanical property parts, the low Young's modulus and high flexibility of the PI HIFY-TENG enable the weft HIFYs close with each other driven by the weaving opening tension (Figure 2i). Owing to the highly stretchability and deformity of weft 3D HIFY yarn, the fabric shows a high stretchability of more than 220% (Figure S14, Supporting Information), which is much higher than the plain structured fabric weaved by normal core–shell structured fabrics.[23,25] Thus, it is worth mentioning that the fancy yarn can get a fancier fabric structure (Figure 4a) only by simple plain weave.

3D HIFY-TENG fabrics can also generate self-powered energy during stretching of the fabric because of the strain-driven deformation of weft yarns. As shown in Figure 4f, the energy output enhances with the fabric strain increases. Moreover, the 3D HIFY fabric shows a unique intelligent porosity adjustment property, owing to the geometric deformation of 3D HIFY yarn (Figure 4h). In detail, when the fabric gets stretched in the weft direction, wing yarns of the adjacent 3D HIFY yarns get straightened, leaving a pore in each fabric structure unit (Figure 4i–j). Therefore, when the 3D HIFY fabric is stretched, the originally close arranged fabric shows an opened porous structure. On the contrary, these opened pores will be closed when the 3D HIFY fabric return to the original state, exhibiting a special intelligent pore adjusting performance. We characterized the porosity by adjusting the optical image threshold via imaging processing, and the results show that the visual porosity can reach 18.2% when the strain was 200% (Figure 4j). Further, we compared the gray values of lines 1 and 2 from the images before and after stretching by ImageJ software, respectively (Figure 4i–j). Because the gray value in the pore parts of the fabric is more than 200, while that in the fiber areas is less, we calculated the line percentage where the gray value is bigger than 200 as the pore parts. Results show that the pore

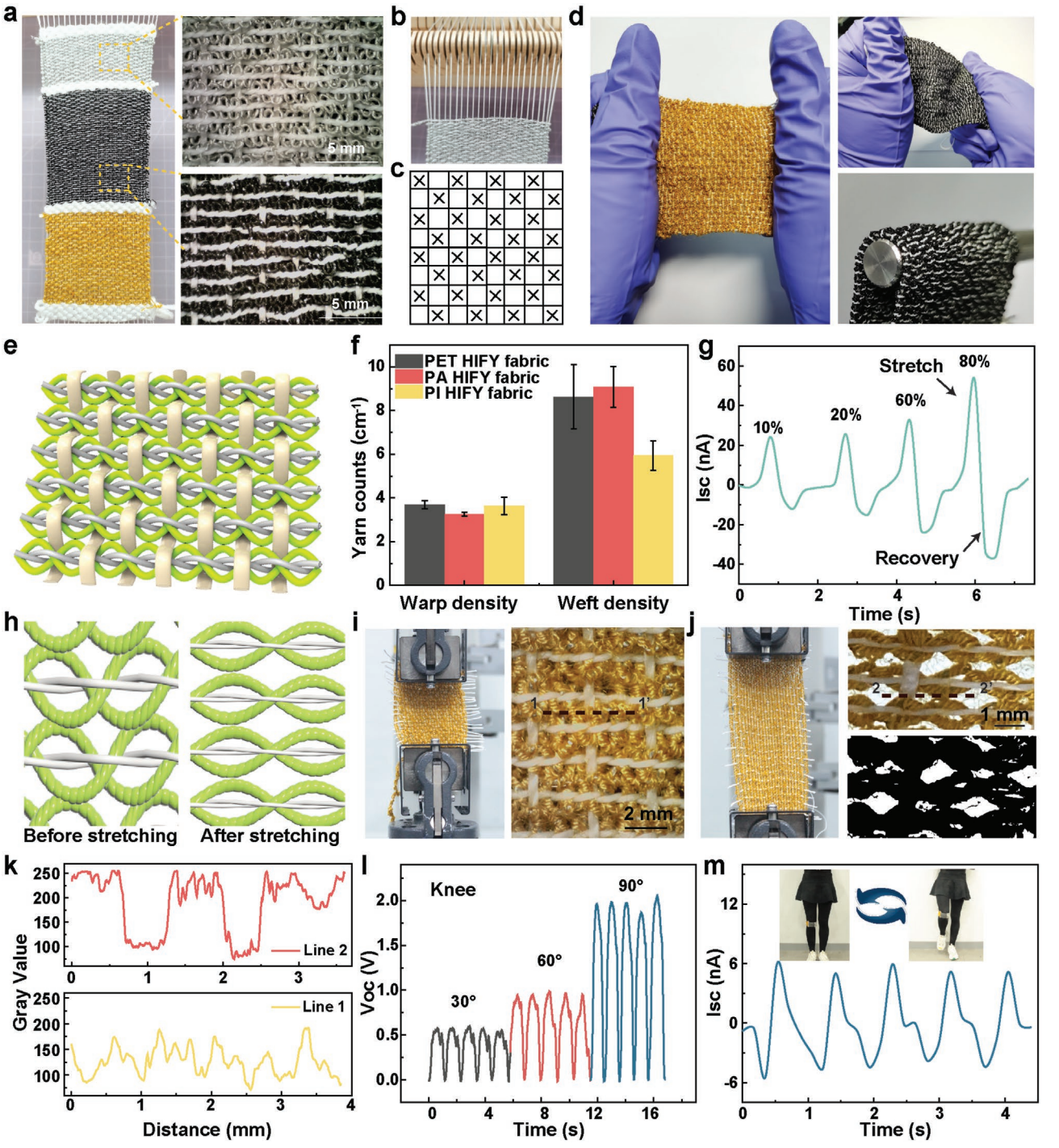

Figure 4. 3D HIFY-TENG fancy fabric weaving for the unique pore effect and energy harvesting. a) Weaving proce ss and products of three kinds of 3D HIFY-TENG fabrics. b) Weaving loom for 3D HIFY-TENG fabrics. c) Plain weaving pattern design for 3D HIFY-TENG fabric. d) Flexibility, bendability, and conformity of 3D HIFY-TENG fabrics. e) Scheme of the 3D HIFY-TENG fabrics. f) Weft and warp density of the 3D HIFY-TENG. g) Electrical output when the fabric was stretched into different strains. h) Illustration of the pore effect of the 3D HIFY-TENG fabric. i) Optical and microscope original 3D PI HIFY-TENG without stretching. j) 3D PI HIFY-TENG when stretched into 200%, showing an obvious pore effect. k) Gray values measured from Line 1 and Line 2. Electrical output of the 3D HIFY-TENG (l) and its fabric (m) during bending when it is fixed on the knee.

parts in line 2 from stretched fabric account for 70%, while that in line 1 from original fabric is 0, as shown in Figure 4k. This further proved the pore effect of 3D HIFY-TENG fabric during stretching. The fancy-yarn with multi-functional composite with novel pattern and delicate style will broaden the application fields of the technical and biomedical textiles.

Due to the good mechanical property, structure stability, conformity, and energy harvesting performance, 3D HIFY

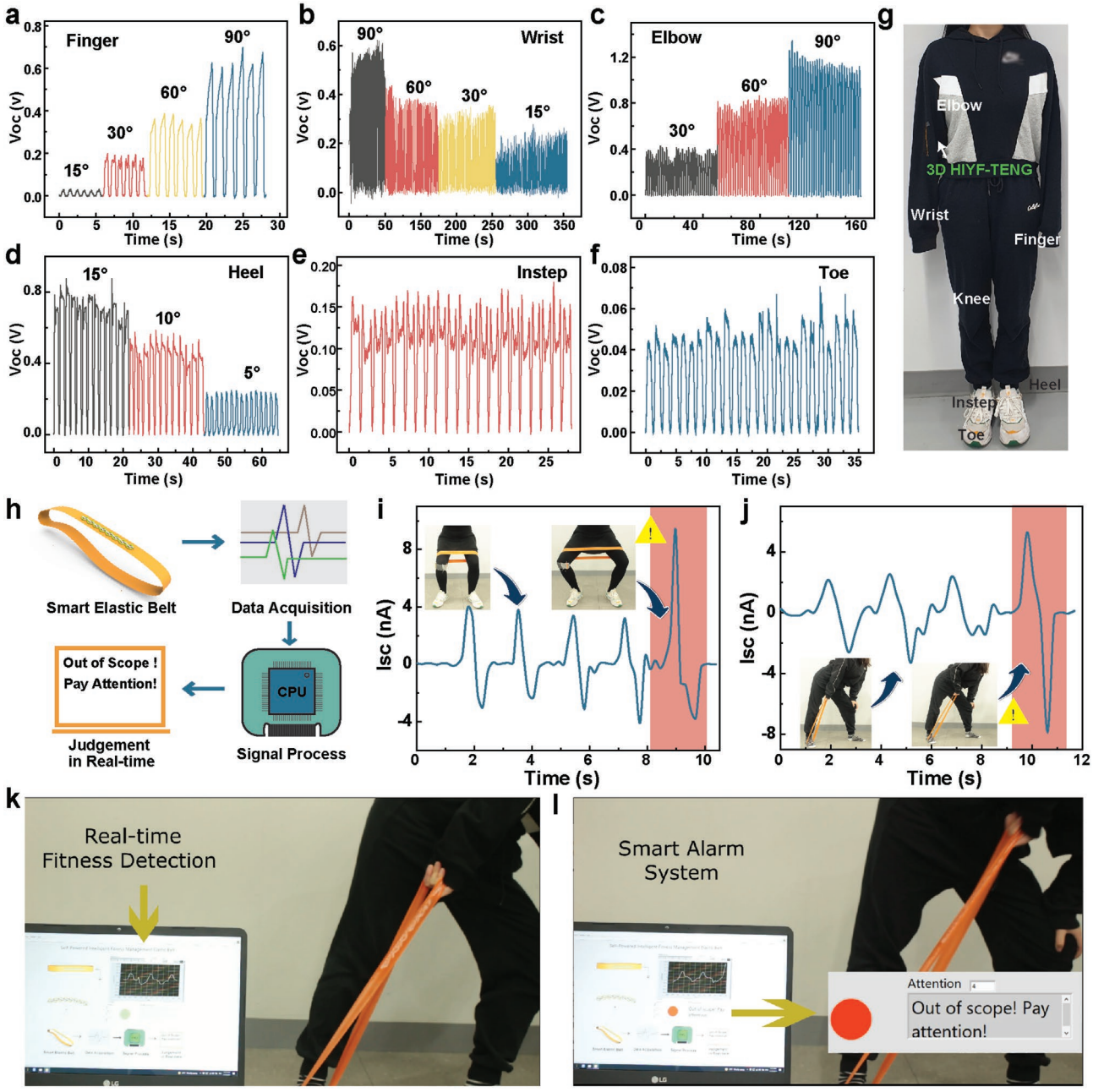

Figure 5. Smart fitness system realized by the intelligent elastic belt embedded with 3D HIFY-TENG. a–f) Human joint movement monitored by 3D HIFY-TENG. g) Photo showing the human body biomechanical energy harvesting from different joints by wearing the 3D HIFY-TENG. h) Scheme of the 3D HIFY-TENG based self-powered smart fitness system. i,j) Self-powered fitness detection and the wrong posture alarming. Demonstration of the smart fitness system for k) real-time fitness detection and l) smart over-stretch alarm system.

fabric can be directly fabricated as smart garments for self-powered human motion detection. As shown in Figure 4l,m, when the 3D HIFY-TENG and 3D HIFY fabric are embedded in the knee joint of the sporting cloth, human motions such as joint bending can be real-time detected because of the stretching of 3D HIFY-TENG. It is worth mentioning that our stretchable self-driven TENG fabric can detect the human motions directly without relying on the substrate materials based on the unique structure deformation of a single 3D HIFY-TENG yarn.

Based on above discussion, the 3D HIFY-TENG can be also used for human bioenergy harvesting from diverse movements of the human body, such as finger, wrist, elbow, heel, instep, and toe bending (**Figure 5**a–g). When the human joints are bent into different degrees, energy outputs from 3D HIFY-TENG gradually increase. In addition, a smart fitness system is further developed for multifunctional exercise management of self-powered real-time exercise detection, exercise frequency statistical analysis, posture correction alarming and energy harvesting by integrating the 3D HIFY-TENG into a smart

yoga belt. As illustrated in Figure 5h, the smart fitness system is composed of smart elastic belt, data acquisition, signal processing mode, and real-time display terminal. The interlocked structure of 3D HIFY-TENG is attached to the yoga belt with double wings distributed in the horizontal direction. Every stretching of the yoga belt led to a friction between the wing yarns of 3D HIFY-TENG with the PU torso yarns and elastic belt, an electrical signal is therefore generated (Figure S15, Supporting Information). Such signals are collected, processed and finally displayed on the display terminal according to the user's purpose and setting in Figure S15, Supporting Information. Our 3D HIFY-TENG based smart fitness system reveals four main functions. First, it can be used for self-powered real-time exercise detection owing to the self-driven 3D HIFY-TENG principle. The smart elastic belt can generate different output of electrical signals depending on the stretching degree (Figure S16, Supporting Information), therefore, the stretching force and displacement of each fitness action can be distinguished and recorded by the smart fitness system. Second, the system can be used for exercise frequency statistical analysis by calculating the electrical signal peaks, because every exercise action will generate one electrical signal. Third, the smart fitness system can be used for over-stretch alarming and posture correction, which is important for body protection from physical danger during fitness. With our system, users can set a personalized alarming value before starting exercise according to the fitness posture type, and once the human body is stretched above the standard value, an alarm signal will be generated, and a "red" light will be triggered. For example, when a volunteer is doing exercises such as squatting or side pulling, once the distance between the legs or limbs exceeds the standard distance, the smart elastic band will give an alarm signal to stop and suggest for correction, so that it will protect the exerciser from physical injury by muscles over stretching (Figure 5i–l), and Video S2, Supporting Information. Forth, the smart elastic belt can harvest energies from human regular fitness, which become a very important and well welcomed human activity. These mechanical energies made by human bodies are normally wasted and it will be very meaningful to be transferred as electrical energies.

3. Conclusion

In summary, we developed a 3D HIFY-TENG with a double-wing structure, for multifunctional energy harvesting modes and self-powered sensing. The unique structure of 3D HIFY-TENG enables it a superior stretchability and deformability, causing the wing yarns contact with the torso yarns, generating self-driven triboelectrical outputs. A numerical model is established to analyze and predict the deformation of 3D HIFY-TENG, which shows consistent with the experimental data. Moreover, the 3D HIFY-TENG shows a robust mechanical property, good stretchability (>350%), weavability, tailorability, conformability, and washability. The 3D HIFY-TENG is further into three kinds of self-powered fabric sensors with a plain structure, which has a much higher stretchability compared with the fabric fabricated with normal core-shell structured yarn TENG using the same weaving structure. The fabric not only shows good performance to the self-powered sensing, but only exhibits a unique adjustable pore effect during stretching, demonstrating an application potential in smart filters. For the application, we developed a smart fitness system by integrating the fancy yarn into a smart elastic belt was developed for multifunctional exercise management of exercise frequency statistical analysis, real-time exercise detection, and self-powered posture correction alarming. This explored systematic work lays the foundation for "multifunctional fashion smart garment".

4. Experimental Section

Materials: Polyimide yarns were purchased from Aoshen Co., Ltd., China. Polyester and polyamide yarns were bought from Alibaba website. Conductive polyamide yarn was brought from Qingdao Zhi Yuan Xiangyu Functional Fabric Co., Ltd., China. Polyurethane yarns were purchased from Zhuji Haoting Chemical Fiber Management Department, Zhejiang, China.

Fabrication of Wing Yarns: The wing yarns were prepared using previous reported fabrication methods by the authors.[23,25] Sheath layer yarns (PI, PET, PA yarn) were first transferred to hollow yarn bobbins from commercial bobbin using QFB650 yarn pressing machine. Then, hollow yarn bobbin and core conductive yarn were mounted on fancy twisting machine (QFB730K) for spinning.

Fabrication of 3D HIFY-TENG: 3D braiding machine (16T-2, Xuzhou Henghui Braiding machine Co., Ltd.) was used for fabricating 3D HIFY-TENG. Torso yarns and wing yarns were mounted on the designated spindles (Figure 1a). The spindle speed was set as 71.5 rpm. The 3D HIFY-TENG fabric was woven by a wood weaving loom (Huan Xi Bei Er, Zhejiang, China). First, the polyamide warp yarns were arranged and warped on the loom; second, the 3D HIFY-TENG yarn was wrapped around the shuttle; then, by feeding the shuttle into the opening of warp yarns (Figure S12, Supporting Information), the fabric was started to be weaved.

Measurements and Characterizations: The morphologies of 3D HIFY-TENG were analyzed by scanning electron microscopy (TM3000, Hitachi Group-Japan) and Dino-Lite digital microscope. The XL-1A yarn strength elongation tester (Shanghai Xinxian Instrument Co., Ltd.) was used to test the mechanical properties of 3D HIFY-TENG. The testing yarn sample was clamped at the crosshead with a gauge length of 20 mm. For the washability test, 3D HIFY-TENG was wound on a shelf and washed in a container with detergent (Figure 3j). Electrical output performances of samples were recorded by electrometer (Keithley 6514). The 3D HIFY-TENG yarns were pasted on the acrylic plate to test the electrical properties. The data collected in human participants study (physiological signal detection and motion tracking) were approved by volunteers and the consent forms are signed.

Supporting Information

Supporting Information is available from the Wiley Online Library or from the author.

Acknowledgements

This work was supported by the National Key R & D Project from Minister of Science and Technology (2021YFA1201601), Open Project Funding of the Key Laboratory of High Performance Fibers and Products, and Science Foundation of Zhejiang Sci-Tech University (20202090-Y).

Conflict of Interest

The authors declare no conflict of interest.

Author Contributions

R.W. and S.L. contributed equally to this work. R.W. and S.L. designed and fabricated the textile TENGs. R.W., L.M., Z.L., and S.Z., characterized the performance. All authors have reviewed and approved the manuscript. L.M. and Z.W. supervised the work. The volunteer (R.W.) agreed to all tests in the manuscript with informed consent.

Data Availability Statement

The data that support the findings of this study are available from the corresponding author upon reasonable request.

Keywords

energy harvesting textile, fancy yarns, hierarchical interlocked yarn, smart fitness systems, triboelectric nanogenerators

Received: April 15, 2022
Revised: June 16, 2022
Published online:

[1] a) T. A. M. Suter, K. Smith, J. Hack, L. Rasha, Z. Rana, G. M. A. Angel, P. R. Shearing, T. S. Miller, D. J. L. Brett, *Adv. Energy Mater.* **2021**, *11*, 2101025; b) K. R. S. D. Gunawardhana, N. D. Wanasekara, R. D. I. G. Dharmasena, *iScience* **2020**, *23*, 101360.

[2] a) H. Ryu, H. J. Yoon, S. W. Kim, *Adv. Mater.* **2019**, *31*, 1802898; b) W. Paosangthong, R. Torah, S. Beeby, *Nano Energy* **2019**, *55*, 401; c) F. Yi, Z. Zhang, Z. Kang, Q. Liao, Y. Zhang, *Adv. Funct. Mater.* **2019**, *29*, 1808849; d) K. R. S. Gunawardhana, N. D. Wanasekara, K. G. Wijayantha, R. D. I. Dharmasena, *ACS Appl. Electron. Mater.* **2022**, *4*, 678.

[3] a) W. Yan, G. Noel, G. Loke, E. Meiklejohn, T. Khudiyev, J. Marion, G. C. Rui, J. N. Lin, J. Cherston, A. Sahasrabudhe, J. Wilbert, I. Wicaksono, R. W. Hoyt, A. Missakian, L. Zhu, C. Ma, J. Joannopoulos, Y. Fink, *Nature* **2022**, *603*, 616; b) A. Libanori, G. R. Chen, X. Zhao, Y. H. Zhou, J. Chen, *Nat. Electron.* **2022**, *5*, 142; c) J. Xiong, P. Cui, X. L. Chen, J. X. Wang, K. Parida, M. F. Lin, P. S. Lee, *Nat. Commun.* **2018**, *9*, 4280; d) S. Dong, F. Xu, Y. Sheng, Z. Guo, X. Pu, Y. Liu, *Nano Energy* **2020**, *78*, 105327; e) R. Wu, L. Ma, A. Patil, Z. Meng, S. Liu, C. Hou, Y. Zhang, W. Yu, W. Guo, X. Liu, *J. Mater. Chem. A* **2020**, *8*, 12665.

[4] a) X. Shi, Y. Zuo, P. Zhai, J. Shen, Y. Yang, Z. Gao, M. Liao, J. Wu, J. Wang, X. Xu, *Nature* **2021**, *591*, 240; b) R. Wu, L. Ma, C. Hou, Z. Meng, W. Guo, W. Yu, R. Yu, F. Hu, X. Y. Liu, *Small* **2019**, *15*, 1901558; c) Y. Zheng, X. Han, J. Yang, Y. Jing, X. Chen, Q. Q. Li, T. Zhang, G. Li, H. Zhu, H. Zhao, G. Snyder, K. Zhang, *Energy Environ. Sci.* **2022**, *15*, 2374; d) R. Wu, L. Ma, S. Liu, A. B. Patil, C. Hou, Y. Zhang, W. Zhang, R. Yu, W. Yu, W. Guo, X. Y. Liu, *Mater. Today Phys.* **2020**, *15*, 100243.

[5] X. Pu, L. X. Li, M. M. Liu, C. Y. Jiang, C. H. Du, Z. F. Zhao, W. G. Hu, Z. L. Wang, *Adv. Mater.* **2016**, *28*, 98.

[6] a) L. Chen, C. Chen, L. Jin, H. Guo, A. Wang, F. Ning, Q. Xu, Z. Du, F. Wang, Z. L. Wang, *Energy Environ. Sci.* **2021**, *14*, 955; b) Y. Hu, Z. Zheng, *Nano Energy* **2019**, *56*, 16; c) R. Wu, L. Ma, X. Liu, *Adv. Sci.* **2022**, *9*, 2103981; d) Z. Zhou, K. Chen, X. Li, S. Zhang, Y. Wu, Y. Zhou, K. Meng, C. Sun, Q. He, W. Fan, E. Fan, Z. Lin, X. Tan, W. Deng, J. Yang, J. Chen, *Nat. Electron.* **2020**, *3*, 571.

[7] a) Z. Chen, R. Wu, S. Guo, X. Liu, H. Fu, X. Jin, M. H. Liao, *Soft Rob.* **2021**, *8*, 226; b) S. Shen, J. Yi, R. Cheng, L. Ma, F. Sheng, H. Li, Y. Zhang, C. Ning, H. Wang, K. Dong, Z. L. Wang, *Adv. Electron. Mater.* **2022**, *8*, 2101130.

[8] A. Yu, X. Pu, R. Wen, M. Liu, T. Zhou, K. Zhang, Y. Zhang, J. Zhai, W. G. Hu, Z. L. Wang, *ACS Nano* **2017**, *11*, 12764.

[9] C. Ye, S. Yang, J. Ren, S. Dong, L. Cao, Y. Pei, S. Ling, *ACS Nano* **2022**, *16*, 4415.

[10] a) D. Zhang, W. Yang, W. Gong, W. Ma, C. Hou, Y. Li, Q. Zhang, H. Wang, *Adv. Mater.* **2021**, *33*, 2100782; b) K. Wang, C. Hou, Q. Zhang, Y. Li, H. Wang, *Nano Energy* **2022**, *95*, 107055; c) H. Chu, X. Hu, Z. Wang, J. Mu, N. Li, X. Zhou, S. Fang, C. S. Haines, J. W. Park, S. Qin, N. Yuan, J. Xu, S. Tawfick, H. Kim, P. Conlin, M. Cho, K. Cho, J. Oh, S. Nielsen, K. A. Alberto, J. M. Razal, J. Foroughi, G. M. Spinks, S. J. Kim, J. Ding, J. Leng, R. H. Baughman, *Science* **2021**, *371*, 494.

[11] a) Y. Mao, Y. Li, J. Xie, H. Liu, C. Guo, W. B. A. Hu, *Nano Energy* **2021**, *84*, 105918; b) Q. Zhang, T. Jin, J. Cai, L. Xu, T. He, T. Wang, Y. Tian, L. Li, Y. Peng, C. Lee, *Adv. Sci.* **2022**, *9*, 2103694.

[12] a) Y. Gao, Z. Li, B. Xu, M. Li, C. Jiang, X. Guan, Y. Yang, *Nano Energy* **2022**, *91*,106672; b) E. He, Y. Sun, X. Wang, H. Chen, B. Sun, B. Gu, W. Zhang, *Composites, Part B* **2020**, *200*, 108244.

[13] P. Wang, J. Zhou, B. Xu, C. Lu, Q. A. Meng, H. Liu, *Adv. Mater.* **2020**, *32*, 2003453.

[14] C. Chen, L. Chen, Z. Wu, H. Guo, W. Yu, Z. Du, Z. L. Wang, *Mater. Today* **2020**, *32*, 84.

[15] a) D. Kim, J. Park, Y. Kim, *ACS Appl. Energy Mater.* **2019**, *2*, 1357; b) Z. Bai, T. He, Z. Zhang, Y. Xu, Z. Zhang, Q. Shi, Y. Yang, B. Zhou, M. Zhu, J. Guo, C. Lee, *Nano Energy* **2022**, *94*, 106956; c) L. Y. Ma, M. J. Zhou, R. H. Wu, A. Patil, H. Gong, S. H. Zhu, T. T. Wang, Y. F. Zhang, S. Shen, K. Dong, L. K. Yang, J. Wang, W. X. Guo, Z. L. Wang, *ACS Nano* **2020**, *14*, 4716.

[16] V. Sanchez, C. J. Walsh, R. J. Wood, *Adv. Funct. Mater.* **2021**, *31*, 2008278.

[17] M. Guo, F. Sun, W. Gao, *Text. Res. J.* **2019**, *89*, 2741.

[18] S. Petrulyte, *Indian J. Fibre Text. Res.* **2007**, *32*, 21.

[19] L. Wang, M. W. King, *Biomedical Textiles*, China Textile Press, Beijing, China **2010**.

[20] M. Alshukur, A. Fotheringham, *J. Text. Inst.* **2015**, *106*, 490.

[21] M. Alshukur, H. Gong, G. Stylios, *Int. J. Clothing Sci. Technol.* **2018**, *30*, 268.

[22] R. Wu, T. Kim, *Lab Chip* **2021**, *21*, 1217.

[23] L. Ma, R. Wu, S. Liu, A. Patil, H. Gong, J. Yi, F. Sheng, Y. Zhang, J. Wang, J. Wang, W. Guo, Z. L. Wang, *Adv. Mater.* **2020**, *32*, 2003879.

[24] C. Chen, Z. Du, W. Yu, T. Dias, *Text. Res. J.* **2018**, *88*, 59.

[25] L. Ma, R. Wu, A. Patil, J. Yi, D. Liu, X. Fan, F. Sheng, Y. Zhang, S. Liu, S. Shen, J. Wang, Z. L. Wang, *Adv. Funct. Mater.* **2021**, *31*, 2102963.